Available online at www.sciencedirect.com
ScienceDirect
Procedia Engineering 2 (2010) 707–716
Procedia Engineering
www.elsevier.com/locate/procedia

Fatigue 2010

Finite elements prediction of thermal stresses in work roll of hot rolling mills

D. Benasciutti[a]*, E. Brusa[b], G. Bazzaro[c]

[a]*Università di Udine, via delle Scienze 208, 33100 Udine, Italy*
[b]*Politecnico di Torino, Dipartimento di Meccanica, Corso Duca degli Abruzzi 24, 10129 Torino, Italy*
[c]*Centro Ricerche Danieli, Danieli Officine Meccaniche S.p.A., via Nazionale 41, 33042 Buttrio (Udine), Italy*

Received 4 February 2010; revised 9 March 2010; accepted 15 March 2010

Abstract

A simplified numerical approach based on finite elements to compute thermal stresses occurring in work roll of hot rolling mills is here proposed. To decrease both the complexity of the analysis and the computational effort, this approach implements a plane finite element model of the work roll alone, loaded on its surface by the rotating thermal actions due to the cyclic sequence of the conductive heating caused by the contact with hot strip and cooling provided by water jets. Results from thermal analysis are preliminary compared to an analytical solution available in the literature and then applied as thermal input in the subsequent mechanical finite elements simulations, which provide thermal stress in the work roll and the elastic-plastic evolution of elements, close to the work roll surface.

Keywords: hot rolling; work roll; thermal stresses; finite elements.

1. Introduction

Work roll in hot rolling mills is simultaneously excited by cyclic thermal and mechanical stresses, respectively. Thermal stresses are caused by a non-uniform temperature distribution over the work roll surface. It is induced by strip heating and water jet cooling, whereas mechanical stresses are produced by rolling pressures and contact actions with back-up rolls. In hot rolling thermal stresses are usually comparable or even larger than mechanical stresses [1, 2, 3]. Thermal stresses in work roll induce both elastic and plastic strains, often leading to some surface damage mechanisms like wear, thermal fatigue and so-called 'spalling', which may produce unexpected failures [1].

In order to predict work roll life and conformingly schedule maintenance operation estimating the actual service loads is strictly required. Thermo-mechanical coupling makes analysis rather difficult. Analytical approaches are impractical and sometimes inapplicable, while numerical approaches, based on the finite element method, look very attractive. To predict the actual behaviour of the rolling mill, some approaches proposed in the literature include into the numerical model both the strip plastic deformation and the thermo-mechanical coupling with work roll. Computational resources and simulation times required appear huge [4,5] and unsuitable for current industrial needs.

* Corresponding author. Tel.: +39-0432-558048; fax: +39-0432-558251.
E-mail address: denis.benasciutti@uniud.it.

1877-7058
doi:10.1016/j.proeng.2010.03.076

Suitable strategies to simplify the analysis, allowing a significant reduction of the overall computation time are currently looked for, although accuracy in modelling is another main goal. This perspective motivates the current interest in investigating the capability of alternative numerical approaches, aimed at reducing the computational burden, while still providing reliable estimates of work roll stresses [6, 7, 8].

In light of the above considerations, this work aims at developing a simplified approach to predict thermal stresses in hot-rolling work rolls, based on the finite element method (FEM). More precisely, analysis assumes a plane finite element model of the work roll by avoiding to model the strip, then effects of rotating heating and cooling thermal fluxes are applied on its surface, to represent the hot strip rolling conditions. Strip plastic deformation, as well as mechanical loads at the interface between work roll and, respectively, strip and back-up roll, are not included in the analysis. Cyclic temperature changes occurring during the hot rolling process are modeled in the local reference frame of the work roll and rotating thermal loads are applied over the work roll surface.

Transient thermal history in work roll is first simulated. It allows identifying the so-called "thermal boundary layer" close to work roll surface, where the largest thermal gradients occur. Numerical results coming from thermal analysis were compared to an analytical solution available in the literature and did show a very good agreement. Results from the thermal transient response are then applied as thermal inputs in the following mechanical simulations. This allows estimating the transient elastic-plastic thermal stresses within the work roll. Numerical results consequently obtained, although preliminary, looked very promising and confirmed that the proposed approach could be a valid tool for estimating work roll thermal stresses, at least in early design phases. An experimental validation of the numerical finite elements model would be required, as well as an experimental evaluation of both thermo-mechanical materials properties and thermal coefficient used in numerical simulations.

2. Thermal stresses in hot rolling work roll

Fig. 1 shows a sketch of the thermal and mechanical loads in hot-rolling work roll. Mechanical loads are confined to the bite region (strip pressures) and to the small contact area between work and back-up rolls, respectively (hertzian pressures). Thermal actions, instead, develop over the entire work roll surface and are induced by conductive heating due to hot strip contact and natural and forced convective cooling provided by air and water jets, respectively. Work roll revolutions then induce a cyclic sequence of heating and cooling phases on the surface, being responsible of cyclic tensile and compressive stresses (Fig. 2(a)). Tangential expansion of roll surface, caused by the heating induced by hot strip contact, is constrained by the surrounding material, which remains at lower temperature. Compressive stresses then arise and may lead to local yielding, depending on the relative temperature gradients between work roll surface and bulk. Tensile stresses, instead, arise in the cooling phase, through a similar and somehow dual mechanism.

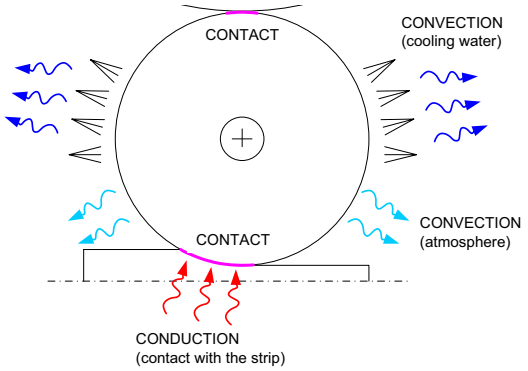

Fig. 1. Thermal and mechanical loads on hot-rolling work roll.

In the literature a simplified method to estimate the thermal stresses and the cyclic elastic-plastic behavior in hot-rolling work rolls has been developed as shown in Fig. 2(b) [2,9]. In the example compressive stresses due to heating (line OA) reach yielding stress at a temperature of 370° (point A). A further temperature increase induces plastic strains and at each temperature compressive stress equals the yielding stress at that temperature (line AB). Subsequent surface cooling produces a tensile stress, first elastic (line BC), then plastic (line CD). The loop closes (line DE) in the subsequent heating.

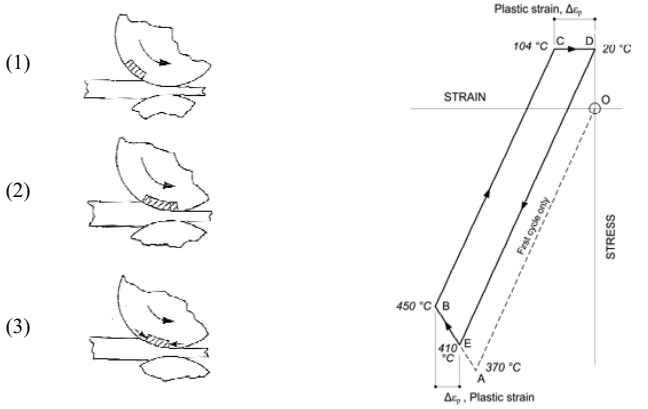

Fig. 2. (a) Stress evolution on work roll surface caused by heating; (b) stress/strain closed loop for a point on work roll surface according to [2].

Roll revolutions are accompanied by an elastic-plastic stress/strain cycles. Plastic strain can be then used in the well-known Manson-Coffin relation to assess the fatigue life [10] as:

$$\Delta\varepsilon_p \sqrt{N} = A \tag{1}$$

where $\Delta\varepsilon_p$ is the plastic strain range, N the number of cycles for surface crack nucleation and A is a material constant. The approach above described, although rather simplified, allows a first approximation estimate of the cyclic stress evolution on work roll surface. A goal of the present paper is to provide more accurate evaluation of thermal stresses by finite element simulations.

3. Analytical solutions for evaluation of stationary temperature distribution

Several papers in the literature provided analytical solutions for the stationary temperature distribution in cylinders, rotating at a constant angular speed under different surface thermal loadings [11,12,13,14,15].

Geometrical configuration herein analyzed resorts to an infinite-width cylinder, rotating at constant angular speed, subjected to a constant heat flux q_0 over the angular sector ϕ and to a convective cooling (with constant heat transfer coefficient h) over sector Ψ, where α is the relative angular distance between the two regions above mentioned, see Fig. 4(a) [11].

For an infinite-width cylinder stationary temperature distribution, which is two-dimensional and uniquely depends on the cylindrical coordinates (r, θ), can be expressed as a Fourier series as follows:

$$\begin{aligned} T(r,\theta) - T_\infty = \quad & b_0 + \sum_{n=1}^{\infty} \left\{ b_n \left[ber_n\left(\sqrt{n\,\mathrm{Pe}}\,\frac{r}{R}\right)\cos(n\theta) - bei_n\left(\sqrt{n\,\mathrm{Pe}}\,\frac{r}{R}\right)\sin(n\theta) \right] + \right. \\ & \left. + c_n \left[ber_n\left(\sqrt{n\,\mathrm{Pe}}\,\frac{r}{R}\right)\sin(n\theta) + bei_n\left(\sqrt{n\,\mathrm{Pe}}\,\frac{r}{R}\right)\cos(n\theta) \right] \right\} \end{aligned} \tag{2}$$

being R and ω radius and angular speed of the cylinder, respectively, while ber_n and bei_n represent the Kelvin functions of order n. Péclet number $Pe=\omega R^2/a$ includes the thermal diffusivity $a=k/\rho c$, expressed as a function of thermal conductivity k, density ρ and specific heat c of the cylinder material.

Equation (2) is a general solution, while series coefficients b_0, b_n, c_n follow from the specific thermal loadings applied on cylinder boundary. As an example, Ref. [11] provides the analytical formulae applicable for constant heat flux and convective cooling, as shown in Fig. 4(a), although literature provide other analytical solutions for different thermal configurations [14,15].

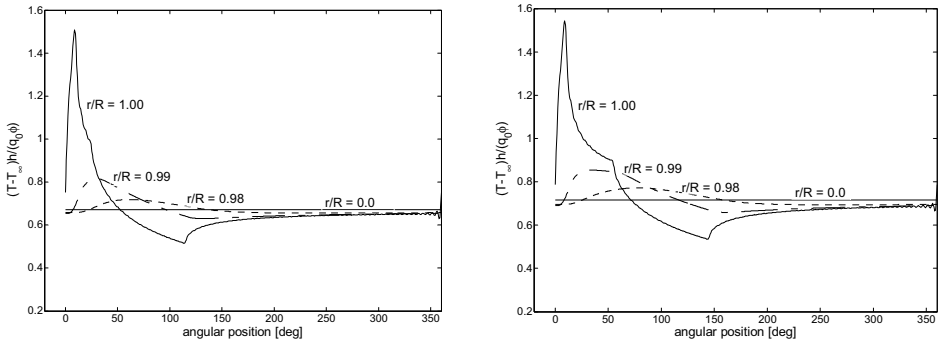

Fig. 3. Analytical temperature distribution at different penetration normalized depths, for configuration shown in Fig. 4(a), with (a) α=15°, (b) α=45°.

Equation (2) has been applied to estimate the temperature distribution as a function of parameter α. Results are coincident with those reported in Ref. [11]. As an example, Fig. 3 shows the distribution of the non-dimensional temperature $(T-T_\infty)h/(q_0\phi)$, where T_∞ is the bulk temperature of the cooling medium, as a function of the angular position θ, for different depths from the cylinder surface and for two angular positions (α=15° and α=45°) of the cooling area (fixed at ϕ=10°, Ψ=90°).

If relative distance between heating and cooling areas increases, a local peak appears at the beginning of the cooling zone. Furthermore, figures above depicted show that thermal gradient is contained within a small depth approximately equal to 6% of the cylinder radius. Under stationary conditions about 94% of the cylinder remains at a fairly constant temperature. This characteristic depth tends to decrease for increasing angular speeds of the roll.

4. Finite element simulations

4.1. Model description

To reduce the overall computational effort and time, a simplified approach is proposed for the numerical investigation. It is based on a plane finite element model of the work roll alone, under the effects of rotating heating and cooling loadings, i.e. the boundary conditions imposed by the hot rolling process. The two-dimensional model, shown in Fig. 4(b) is characterized by an axis-symmetric mapped mesh, with 6940 elements and 6921 nodes, respectively.

As it was emphasized in previous paragraph, the largest temperature gradients within work roll develop near the surface. Therefore, the mesh detailed in Fig. 4(b) shows a decreasing element size close to work roll surface, both along the tangential and radial directions, for a depth of 2% of work roll radius. Numerical investigations are performed by the commercial software ANSYS® and APDL (Ansys Parametric Design Language) script language.

Analysis aims to compute the transient temperature distribution first in work roll under the thermal boundary loadings shown in Fig. 4(a) and then the resulting thermal stresses. Analyzed configuration represents a cylinder with radius R=300 mm, which rotates at a constant angular speed of 28,2 rpm. Work roll is under a constant thermal

flux q_0 over the ϕ=10° angular sector and a convective cooling over the Ψ=90° sector, where α=45° is the relative angular distance between heating and cooling zones, see Table 1.

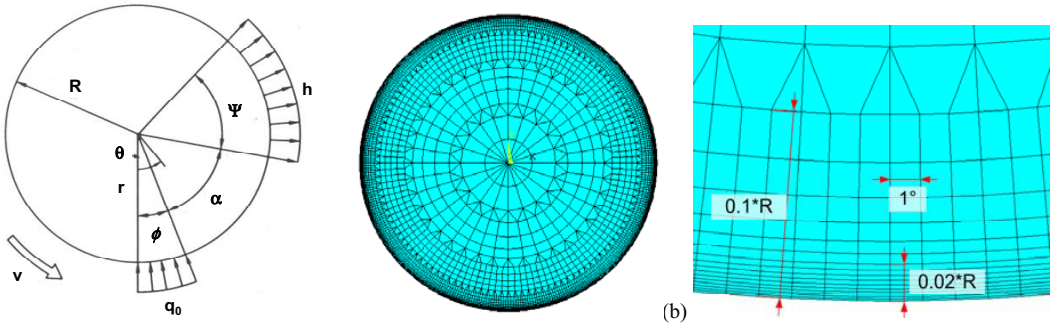

Fig. 4. (a) Thermal configuration analyzed (from [11]), (b) finite elements model (global and zoom).

Table 1. Geometrical and thermal parameters characterizing the configuration shown in Fig. 4(a), which are used in numerical simulations.

Parameter	Description	Value
R	Cylinder radius	300 mm
ω	Angular speed of cylinder	2,953 rad/sec (28,2 rpm)
ϕ	Heating sector	10°
α	Angular gap between heating and cooling	45°
Ψ	Cooling sector	90°
q_0	Input thermal flux (heating)	$13{,}7 \cdot 10^6$ W/m^2
h	Convection coefficient (cooling)	10100 W/m^{2}K
T_0	Bulk temperature of cooling medium	20 °C
T_{roll}	Initial work roll temperature	20 °C

4.2. Thermal analysis

Thermal analysis is based on four-nodes linear thermal elements and assumes temperature-invariant thermal properties for work roll material. Cyclic evolution of heating and cooling thermal loadings, induced by work roll revolutions, is simulated by applying rotating thermal loadings on work roll at rest. As a first approximation, thermal radiation is neglected to keep the analysis linear.

Based on the total amount of elements on the mesh surface (see Fig. 4(b)), a complete work roll revolution is completed after 360 simulation steps. Thermal analysis simulates a time transient of 3600 seconds. It operates through an implicit solver based on the Jacoby Conjugate Gradient (JCG), which looked to be particularly quick and effective for this investigation.

Table 2. Thermal and mechanical properties of the work roll material used in numerical simulations.

Parameter	Description	Value
k	thermal conductivity	90,9 W/mK
ρ	density	7800 kg/m^3
c	specific heat	450 J/kgK
β	thermal expansion coefficient	$11 \cdot 10^{-6}$ K^{-1}
σ_s	yielding stress	500 MPa
E	Young modulus	206000 MPa
ν	Poisson coefficient	0,33

A critical issue of the analysis consists of the accurate selection of all the thermal parameters deserving as input for the numerical simulation, being their experimental identification often rather difficult [16]. A typical example is selecting a suitable value of the input thermal flux. A wide range of values is usually suggested in the literature. For hot rolling of steel, a typical value is $30 \cdot 10^6$ W/m^2, but values as large as $200 \cdot 10^6$ W/m^2 are even compatible with industrial practice. For hot rolling of aluminum, a suggested average value is $10 \cdot 10^6$ W/m^2. Even convection coefficient of water jet cooling may be difficult to be found. Several values can be read in the specialized literature. It depends on the water temperature (with or without boiling), water speed at nozzles and work roll angular speed [17]. A surface temperature upon work roll below 100 °C (without boiling) can be associated to a value of 11000 W/m^{2}K and even up to 40000 W/m^{2}K for a surface temperature above 100 °C (with boiling). In this work a convection coefficient h=10100 W/m^{2}K has been considered suitable, if compared to the industrial practice [18]. For work roll material, temperature-independent properties typical of steel have been assumed, as it can be read in Table 2.

Péclet and Biot numbers can be computed according to values of Table 2:

$$Pe = \frac{\omega R^2}{a} = \frac{2{,}953 \cdot (0{,}3)^2}{2{,}658 \cdot 10^{-5}} = 10^4 \qquad Bi = \frac{h\,R}{k} = \frac{10100 \cdot 0{,}3}{90{,}9} = 33{,}3 \tag{3}$$

where a=2,658·10^{-5} m^2/s is the thermal diffusivity. Péclet number compares the work roll angular speed to its geometrical and thermal parameters in a normalized ratio, whereas the Biot number quantifies the relative ratio of convective and conductive thermal fluxes. Values listed in Eq. (3) are typical of a hot rolling condition.

Figure 5 shows the evolution of the temperature distribution in work roll within the thermal transient of 3600 seconds analyzed. Some consecutive time instants are depicted. Heating and cooling areas are located as in Fig. 4(a). As it can be seen, the maximum thermal gradient is very close to the work roll surface, although a progressive heating near centre is evenly observed.

In Figure 6(a) temperature distribution of points located on work roll surface are represented as a function of the angular variable θ. They were computed for subsequent time instants within the thermal time transient previously analyzed. The same figure even plots the stationary temperature distribution calculated through the Patula's model, reviewed in Section 3.

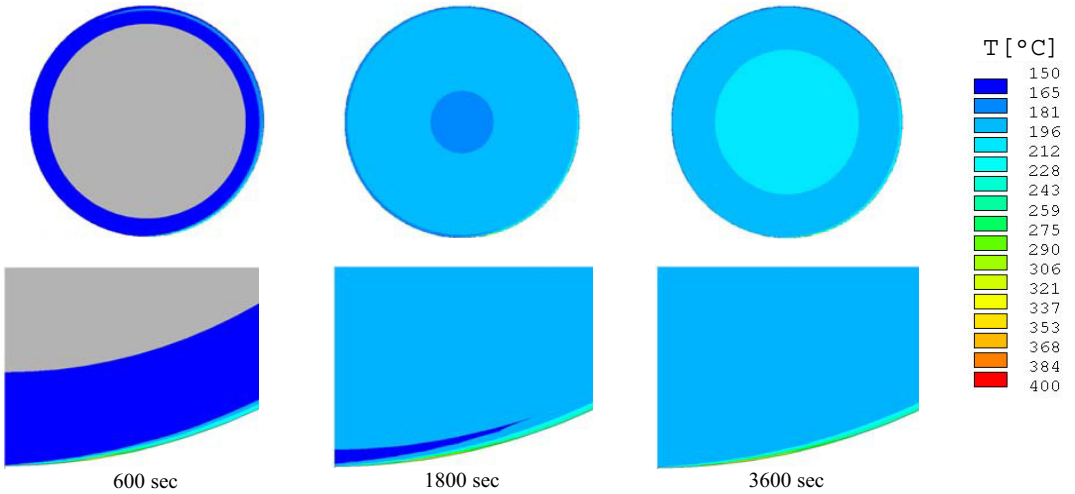

Fig. 5. Temperature change within work roll at consecutive time instants (600, 1800, 3600 sec). Grey areas represent temperatures below 150 °C.

A sharp temperature increase is observed within the heating zone (θ=270°÷280°), followed by a smooth temperature decrease caused by air convection cooling, followed by a more evident temperature drop within the water jet cooling zone (θ = –35°÷55°). It is also worth noting that temperature distribution actually remains quite similar over time, although temperature values grow up. For the configuration here analyzed, just after 1800 seconds (value comparable with [2]) results from numerical simulations converge and practically coincide with the stationary temperature distribution, which is solution of the Patula's model.

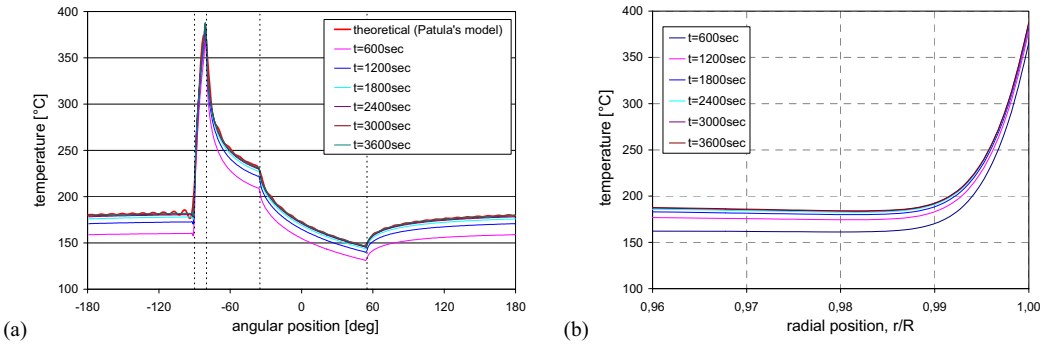

Fig. 6. Temperature distribution within work roll over time, described as a function of: (a) the angular position, (b) the radial position.

Figure 6(b) shows temperature variation along the radial direction, at subsequent time instants. It confirms the existence of a thermal boundary layer close to the work roll surface with a radial depth of approximately 1% of work roll radius, in which the maximum thermal gradients and the largest temperatures are observed.

Figure 7(a) shows the temperature change at work roll surface for a thermal time transient of 60 seconds, while Fig. 7(b) describes points at different radial depths, along the same radius. It confirms results observed in Fig 6(b), but further emphasizes how the largest temperature variation occurs very close to the work roll surface. In the same figure it can be even seen a "thermal inversion" phenomenon induced by forced convection cooling. This action imposes to the points on work roll surface lower temperature values than at some inner points. This phenomenon shall be taken into account when stress distribution on work roll surface will be calculated by means of FEM in the next section.

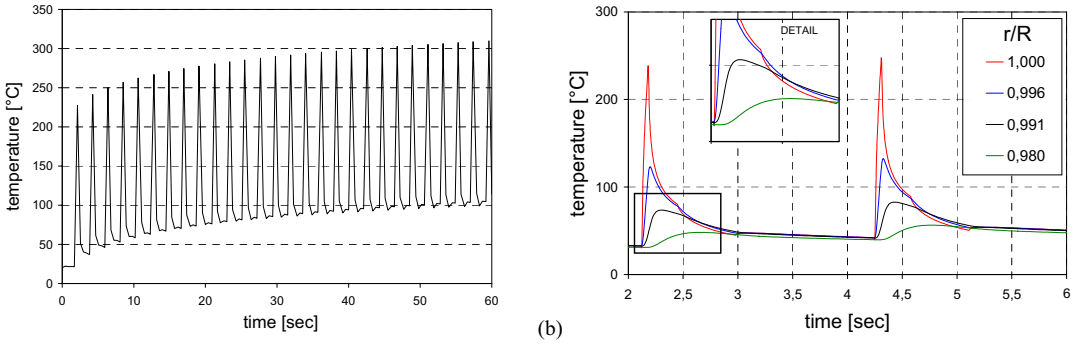

Fig. 7. (a) Thermal time transient of 60 seconds for point on work roll surface; (b) thermal time transient at different radial depths.

5. Mechanical analysis

Numerical results of the time transient thermal analyses are then applied as thermal loads in the following mechanical simulation by means of the so-called "load transfer" method available in ANSYS®. Four-node linear finite elements in plain strain have been used. For work roll material, an elastic-plastic kinematic hardening model has been assumed.

To perform a non-linear solution, the modified Newton-Raphson algorithm has been applied with convergence criteria set on both displacement and force and through an explicit solver code. Compared to thermal simulations, mechanical analyses required larger computation time, at least of an order of magnitude longer.

Results in Figure 8 show circumferential normal stresses within work roll for given time instant, assuming thermal boundary conditions (heating and cooling) imposed according to Fig. 4(a). Stress state looks globally symmetrical with respect to the work roll axis, but it shows a local gradient close to the surface, uniquely along the rolling arc. As it was already observed in thermal analysis, to the cooling and heating regions correspond compressive and tensile stresses, respectively.

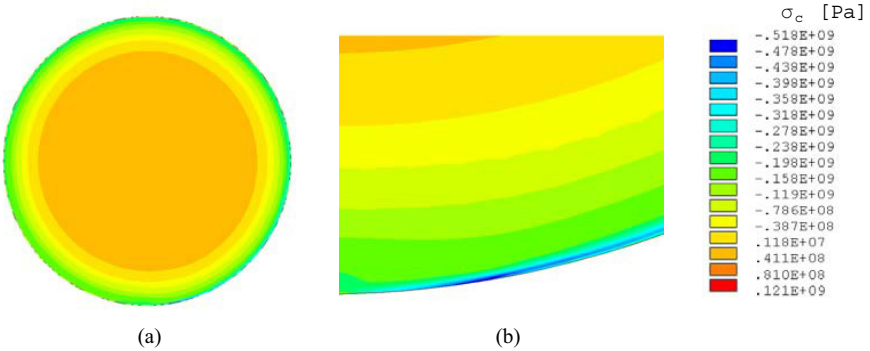

Fig. 8. Circumferential normal stresses on work roll: (a) global view; (b) zoom on the roll bite region.

Further details are provided in Fig. 9(a), which shows the distribution of radial, circumferential and axial stresses on work roll surface, as a function of angular coordinate θ. Radial stress is actually zero, while circumferential and axial stresses, whose amplitude is almost coincident, significantly vary within the range of angular position. Compression occurs in the heating zone (θ =270°÷280°) while tension occurs in the cooling zone (θ = –35°÷55°).

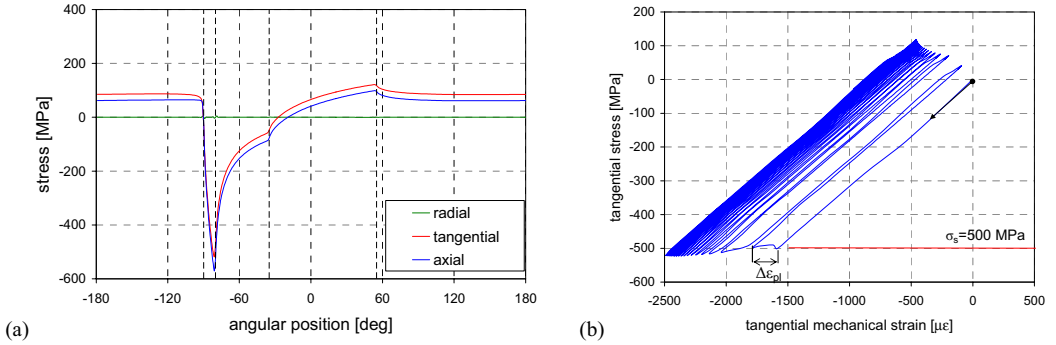

Fig. 9. (a) Stresses on the work roll surface, described as a function of the angular coordinate; (b) circumferential stress vs. strain over time.

The most appreciable result from the point of view of fatigue life prediction is depicted in Fig. 9(b). It shows the time evolution of the circumferential stress and strain, during the first 20 revolutions of work roll. Pattern looks

quite similar to the one sketched in Fig. 2, but work roll configuration herein analyzed shows yielding only in the compressive part of the diagram. Moreover, plastic strain increment decreases at each revolution.

Thermo-mechanical simulations clearly point out that work roll surface is affected by a biaxial stress state, more complex than that the case described in Par. 2 and shown in Fig. 2. This aspect is relevant in case of fatigue life prediction, since it requires the implementation of a suitable approach, which has to resort to both the multi-axial and low cycle fatigue methods.

6. Conclusions

This work proposes a simplified approach to compute thermal stresses in work roll of hot rolling mills, based on a plane finite element model of the work roll alone, subjected on its surface to heating and cooling thermal loads.

Results of the thermal analysis for a time transient of 3600 seconds did show that the largest thermal gradients develop within a small region close to work roll surface, which can be considered like a "thermal boundary layer", if compared to gasdynamics. Temperature distribution computed by the thermal simulations shows a good agreement with results obtained by a theoretical solution available in the literature (Patula's model).

Results from thermal analysis are then used as thermal loads and inputted in the following coupled-field thermo-mechanical simulations. Thermal stresses and elastic-plastic strain evolution over time are then computed at least on work roll surface. A significant result of the numerical investigation is that at each work roll revolution the roll surface looks affected by cyclic stresses, compressive in the heating zone and tensile in the cooling zone, respectively.

Presented approach is obviously a preliminary investigation, whose contribution is more methodological than quantitative. A numerical simplified procedure has been implemented and tested, by comparing some results to the available numerical investigations present in the literature. Actually, this approach looks quite promising, since it avoids analyzing the strip behavior in hot rolling, is able to catch relevant phenomena induced by heating and cooling operations and identifies the thermo-mechanical coupled behavior of the roll material, which was poorly investigated in the literature. Nevertheless, a deep experimental validation of this numerical model is strictly needed. It requires a very complex experimental set up, which is rather difficult to be completed on existing hot rolling mills, daily used in production. In particular, validation has to identify quite precisely the thermal and mechanical properties of work roll material, thermal coefficients and temperature distribution on rolls to allow a suitable model updating.

The proposed model should be used as a tool in the most challenging aspect of this research activity, concerning the identification of the damage mechanisms in work roll. Interaction among wear, fatigue and corrosion is currently unknown while identifying the predominant failure mode occurring in the work roll is required to predict its life. This goal requires an innovative experimental activity, suitable to superimpose those effects and to correlate their role on the material strength, depending on the thermal and mechanical boundary conditions applied as well as on the scale of the monitored mill.

References

[1] Williams RV, Boxall M. Roll surface deterioration in hot strip mills, *J Iron Steel Inst* 1965;**203**:369-77.

[2] Stevens PG, Ivens KP, Harper P. Increasing work-roll life by improved roll cooling practice. *J Iron Steel Inst* 1971;**209**:1-11.

[3] Chang DF. Thermal stresses in work rolls during the rolling of metal strip. *J Mater Process Tech* 1999;**94**:45-51.

[4] Galantucci LM, Tricarico L. Thermo-mechanical simulation of a rolling process with a FEM approach. *J Mater Process Tech* 1999;**92-93**:494-501.

[5] Sun CG, Yun CS, Chung JS, Hwang SM. Investigation of thermomechanical behavior of a work roll and roll life in hot strip rolling. *Metall Mater Trans A* 1998;**29A**:2407-24.

[6] Li CS, Liu XH, Wang GD, He XM. Three dimensional FEM analysis of work roll temperature field in hot strip rolling. *Mater Sci Tech* 2002;**18**:1147-50.

[7] Li CS, Yu HL, Deng GY, Liu XH, Wang GD. Numerical simulation of temperature field and thermal stress field of work roll during hot strip rolling. *J Iron Steel Res Int* 2007;**14**(5):18-21.

[8] Lee JD, Manzari MT, Shen YL, Zeng W. A finite element approach to transient thermal analysis of work rolls in rolling process. *J Manuf Sci Eng, Trans ASME* 2000;**122**:706-16.

[9] Saha JK, Kundu S, Chandra S, Sinha SK, Singhal U, Das AK. Mathematical modelling of roll cooling and roll surface stress. *ISIJ Int* 2005;**45**(11):1641-50.

[10] Manson SS. *Thermal stress and low-cycle fatigue*. McGraw-Hill; 1966.

[11] Patula EJ. Steady-state temperature distribution in a rotating roll subject to surface heat fluxes and convective cooling. *J Heat Transf* 1981;**103**:36-41.

[12] Yuen WY. On the steady-state temperature distribution in a rotating cylinder subject to heating and cooling over its surface. *J Heat Transf* 1984;**106**(3):578-85.

[13] Fischer FD, Schreiner WE, Werner EA. The temperature and stress fields developing in rolls during hot rolling. *J Mater Process Tech* 2004;**150**:263-69.

[14] Tseng AA, Tong SX, Maslen SH, Mills JJ. Thermal behavior of aluminum rolling. *J Heat Transf* 1990;**112**:301-8.

[15] Tseng AA, Tong SX, Chen TC. Thermal expansion and crown evaluations in rolling processes. *Mater Design* 1997;**18**(1):29-41 (erratum of paper published in *Mater Design* 1996;**17**(4):193-204).

[16] Tseng AA: Thermal modeling of roll and strip interface in rolling processes: Part 1 – Review. *Numer Heat Transfer, Part A* 1999;**35**:115-33.

[17] Tseng AA, Lin FH, Gunderia AS, Ni DS. Roll cooling and its relationship to roll life. *Metall Trans A* 1989;**20A**:2305-20.

[18] Tseng AA. A numerical heat transfer analysis of strip rolling. *J Heat Transf* 1984;**106**:512-17.